RF Sensor for Non-invasive Cardiopulmonary Monitoring

Andrea Serra[1], Ruggero Reggiannini[1], Riccardo Massini[2], and Paolo Nepa[1]

[1] Dept. of Information Engineering, University of Pisa,
Via G. Caruso 16, 56122, Pisa, Italy
{andrea.serra,r.reggiannini,p.nepa}@iet.unipi.it
[2] CUBIT scarl
Via Giuntini 13, 56023 - Navacchio di Cascina, Pisa, Italy
riccardo.massini@cubitlab.com

Abstract. Cardiopulmonary information can be extracted from the temporal variations of the input reflection coefficient of a single wearable antenna placed in close proximity of the human thorax. In a previous paper, the authors have shown the potentials of such non-invasive measurement technique through experimental results; as a proof of concept, phase samples were collected by using a Vector Network Analyzer, and conventional non-linear filtering techniques were used to isolate the spectral components related to heartbeat and respiration rate. To get more realistic measurement data, a first prototype of a low-cost RF sensor has been implemented, and improved algorithms have been developed to estimate both heartbeat and breathing rate. Preliminary measurement results are shown to validate the approach, and the effects of the human body movements are discussed.

Keywords: beat rate measurements, non-invasive cardiopulmonary RF sensor.

1 Introduction

Microwave Doppler radars have been suggested as non-contact devices for non-invasive vital signs sensing since 1970s [1]-[4]. The quasi-periodic chest movements induced by the cardiopulmonary activity determine a phase modulation of an electromagnetic wave reflected by (or transmitted through) the human thorax; then through optimized signal processing techniques applied to the demodulated signal, heartbeat and breathing rates, as well as heart rate variability, can be extracted.

A novel non-invasive RF measurement approach has been proposed in [5]-[6] for non-contact measuring of both heartbeat and breathing rate, which makes use of a single wearable antenna close to the body surface. Basically, it has been demonstrated that quasi-periodic movements induced by the cardiopulmonary activities affect the input impedance of the antenna, when the human thorax occupies most of the antenna near field region. To validate the methodology, a preliminary measurement campaign using a Vector Network Analyzer (VNA) was set up; measurements were taken at different frequencies in the UHF band, during regular breathing activity. The col-

B. Godara and K.S. Nikita (Eds.): MobiHealth 2012, LNICST 61, pp. 332–340, 2013.

lected signal (namely samples of the phase of the antenna reflection coefficient recorded in a temporal interval of some tens of seconds) was analyzed in the frequency domain in order to extract the desired spectral components. The respiration information was clearly and promptly detectable as breathing variations affect appreciably the collected signal, while the heartbeat frequency component was not so perceptible. Therefore a deeper analysis was necessary to isolate the heartbeat-induced spectral component; as a first attempt, two conventional non-linear filtering techniques have been checked. Although the proposed method employs an RF transmitting antenna, the authors believe that the physical principle used to achieve vital signs sensing is different from the Doppler effect [1]-[4]. The effectiveness of this novel approach has been confirmed by recent results in [7]-[10].

In this context, the primary goal of this paper is to demonstrate the feasibility of a simple low-cost hardware solution for the RF sensor based on the approach outlined in [5]-[6], for detection and monitoring of both heartbeat and respiration rate. As far as signal processing is concerned, the main enhancement proposed here with respect to the technique in [5]-[6] is the application of a recursive minimum mean square error (Kalman) tracker for estimation of the signal low-frequency (pulmonary) component. It is shown that this technique permits a more reliable extraction and elaboration of the weaker cardiac spectral component.

2 Measurement Set-Up and Phase-Detector Implementation

This section describes the device used for the acquisition of the samples of the reflection coefficient phase of an antenna in close proximity of the human thorax. In the proposed method the antenna must be located as close as possible to the human body (a direct contact is not required, and the antenna can operate through clothing), while Doppler radar prototypes have been always tested with the antenna at a distance of around 0.5-1m from the body. The RF sensor has been designed and built at CUBIT laboratories (Consortium UBIquitous Technologies, Pisa, Italy). Basically, the device is a reflectometer that measures the magnitude ratio and phase difference of signals that are incident on and reflected from a load (in this case the load is represented by the antenna placed in the chest proximity). The analog voltage outputs, representing the two above quantities, are sampled and stored with a sample rate less than 100 Hz (high enough, however, in view of the speed of typical person movements). Processing of the collected data allows to measure the time-varying phase of the antenna reflection coefficient, from which it is possible to extract information about the heartbeat and respiratory rates. Since above phase variations are of the order of tenths of a degree, the measurement device must be capable to detect variations at least one order of magnitude lower. Fig. 1 shows the block diagram of the device that has been prototyped. Preliminary measurements in different frequency bands (400 MHz, 800 MHz, 1500 MHz) showed that lower frequencies can provide larger phase variations (i.e., a higher system sensitivity) [6]; this is in contrast with Doppler-based sensor technology where instead high frequencies are preferred. The realized prototype operates in the ISM band at 433 MHz. Fig. 2 shows a photo of the device. The device uses

an oscillator with an output level of about 6 dBm, which feeds the antenna. A pair of directional couplers test the incident and reflected signals and send them to the inputs of a Gain and Phase Detector (GPD), which produces two analog voltages proportional to the magnitude ratio and phase difference of the incident and reflected signals.

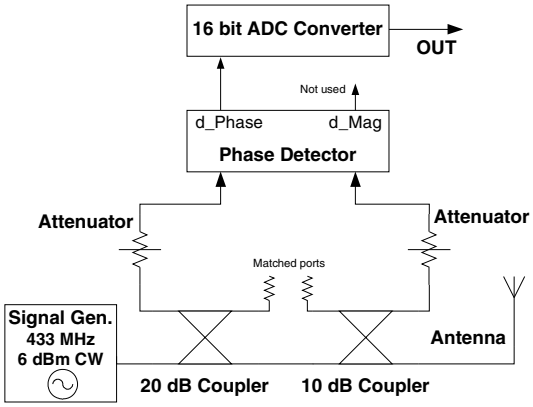

Fig. 1. Block diagram of the device used to get samples of the phase of the reflection coefficient of a wearable antenna

The estimated amplitude of the reflection coefficient is less than -10 dB since the antenna is matched at the working frequency; to approximately balance the level of the two signals at the GPD input, the two directional couplers have different coupling coefficients (20 dB for the incident signal and only 10 dB for the reflected one). Furthermore, the two attenuators set the signal levels around the middle of the GPD dynamic range.

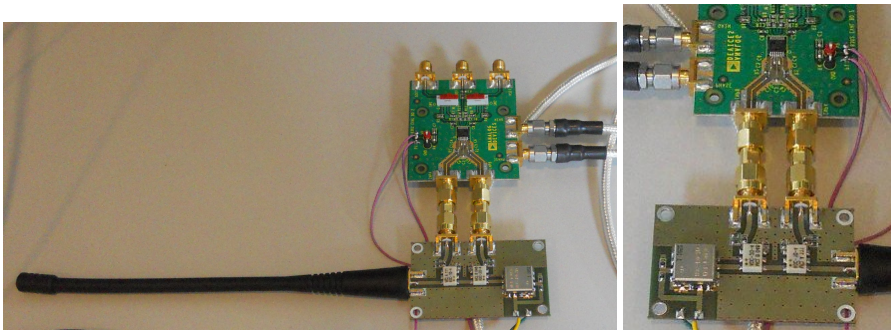

Fig. 2. The RF sensor prototype: the signal generator and the two directional couplers are clearly visible within the PCB (4cmx6cm) at the bottom side of both photos. The Gain and Phase Detector (GPD) based on the AD8302 log detector from Analog Devices is at the top side of the photos.

The GPD is based on the AD8302 log detector from Analog Devices, which produces output voltages in the range 0-1.8 V, with a slope of 10mV/deg. Since it is re-

quired to resolve a hundredth of degree of phase change, a voltage resolution of at least one tenth of mV is needed, which can be obtained by a 16-bit A/D converter with +/-2V input range. To increase the signal-to-noise ratio, the output signal is low-pass filtered. Since in this application only the phase variations must be monitored, it is not necessary to perform a calibration usually required to exclude a measurement setup bias. The only care to be taken is to avoid having a starting value of the phase difference in the proximity of 0 ° or 180 ° values, where the phase detector exhibits a dead zone. It is worth noting that a standard monopole has been used as an antenna. This is possible since the performance of the proposed method does not depend significantly by the antenna shape and technology [6]. This means that an ordinary wearable antenna can be used (in a practical implementation, this latter could be the antenna of a communication device already worn by the user!).

3 Algorithm Description and Performance Analysis

As mentioned earlier, the adoption of a low-cost wearable sensor prompted us to seek and test powerful algorithms capable of a more accurate separation of the pulmonary and cardiac components of the input signal, as compared to those utilized in the previous related literature [6]. Specifically, here we focus on recursive minimum mean square error (MMSE) estimation, or Kalman filtering, for accurate extraction of the signal components slower than the cardiac waveform. The idea behind this approach is similar to that already pursued in [6], i.e., we first try to get as accurate an estimate as possible of the slower-than-cardiac signal fluctuations (dominated by the pulmonary track) and then, as a next step, we proceed removing the cited slow components from the observed data so as to improve the visibility of the (tiny) cardiac waveform over the remaining disturbance, represented by low-frequency residual components, wideband noise and interference. We show that the above MMSE-track-and-subtract approach permits to significantly improve the detectability of the cardiac waveform over previously proposed techniques, such as those in [6].

The MMSE filter was implemented assuming the signal component to be tracked is generated by a linear stationary system described by two state variables, namely, the parameter to be tracked $x(t)$ and its derivative, governed by the same state equations as a simple one-dimensional mechanical system represented by a point mass of position $x(t)$ subject to a random acceleration. Using discrete-time representation with sample spacing T_s, the system inherent state evolution is assumed of the type

$$\mathbf{x}_k = \mathbf{F}\mathbf{x}_{k-1} + \mathbf{w}_k, \quad k = 1, 2, \cdots, N \ , \tag{1}$$

N being the observation length and $\mathbf{F} = \begin{bmatrix} 1 & T_s \\ ; & \\ 1 & 1 \end{bmatrix}$ the state transition matrix, while $\mathbf{w}_k$ indicates the vector noise process, generated assuming that the second derivative of $x(t)$ is zero-mean white Gaussian noise (WGN) with variance σ_p^2.

As for the observations, we assume the following linear time-invariant model:

$$\mathbf{z}_k = \mathbf{H}\mathbf{x}_k + \mathbf{v}_k, \quad k = 1, 2, \cdots, N \ , \tag{2}$$

where $\mathbf{H} = [1 \quad 0]$ and the single real-valued component $\mathbf{v}_k$ is the observation noise, modeled as zero-mean WGN with variance σ_n^2. We observe that parameters σ_n^2 and σ_p^2 have to be jointly calibrated on a trial-and-error basis so as to have the above models fit the level and quality of disturbance affecting the experimental data. The Kalman filter was implemented in Matlab© environment using a conventional formulation [11] and applied to experimental data blocks collected either in the presence or in the absence of respiratory activity as well as body motion of the cooperating subject. The results presented here are only relevant to the subject breathing normally, as the apnea condition was deemed to be unrealistic in an operating scenario. The sampling frequency used to collect the phase of the reflection coefficient is $f_s = 1/T_s = 50$ Hz. The data block size is around 10000 samples, corresponding to a length of 3-4 minutes. Prior to being fed to the Kalman filter, the arithmetic mean of the block is calculated and removed from the data set. Next, the sequence produced by the filter is subtracted from the input block, so as to attempt canceling the slowly-varying components from the input signal. The sequence emerging from the above cancellation procedure eventually undergoes spectral analysis aimed at revealing the most significant residual narrowband components. The analysis software allows to select the segment of time in the input data block to be processed. This can either coincide with the whole block length except for an initial interval (of arbitrary length) containing the filter transient response, or any fragment of the record whatever, presenting features of interest. Spectral analysis is carried out by estimating the signal power spectrum via the periodogram method. The block of experimental data to be analyzed is subdivided into segments ("windows") of equal length, then for each segment the squared modulus of the discrete Fourier transform (DFT) is calculated via the Fast Fourier transform (FFT) algorithm and finally the resulting sequences are averaged. This approach offers a twofold advantage: on one side, it permits to control the spectral analysis resolution, that for the application at hand does not need to be extremely narrow, but compatible with the bandwidth occupancy of the cardiac signal, that is nonzero because of the physiological fluctuations of the heartbeat period. Moreover, to relieve complexity it seems reasonable that the above resolution is chosen not to be far smaller than the maximum tolerable error in the measurement of the cardiac rate. Assuming that the latter is estimated by simply reading the position on the frequency axis of the bin where the periodogram peaks, it turns out that the maximum absolute estimation error is equal to half the spectral resolution. Collecting the above criteria, the resolution should be chosen so as to neither exceed twice the tolerable error in the cardiac rate, nor to be smaller than the cardiac rate instability. The curves presented in this section were produced using 512-point windows, corresponding to a frequency spacing between DFT samples of around 0.1 Hz, i.e. a maximum absolute frequency error of 0.05 Hz, or plus or minus three beats per minute. If this inherent uncertainty seems excessive, it can be considerably reduced by resorting to some form of interpolation on the DFT samples. However the above choice for the resolution allows to safely separate the cardiac from the respiratory components, since these are considerably spaced apart. The second advantage implicit in the above mentioned segmentation of the experimental data blocks stands in the possibility of averaging the partial

spectral estimates originating from the single segments, thus obtaining a significant reduction of the fluctuations due to the random disturbance affecting the signal. Using 512-point windows and data block lengths in the order of 10,000 samples permits to average over some twenty spectral estimates, with a reduction of 4-5 times of the RMS disturbance. The figures presented below were obtained after a calibration of the parameters σ_p^2 and σ_n^2 involved in the dynamic models implicit in the Kalman tracker. A combination that proved to be nearly optimal for most of the available experimental data is $\sigma_p = 0.004 \div 0.006$ and $\sigma_n = 0.1 \div 0.2$. The actual selection for these parameters is specified in the figure captions below. In Figs. 3-4, we present numerical results for two blocks of data (identified as Block #*i*, *i*=1, 2), the first relevant to the cooperating subject standing still and normally breathing, the second with the addition of wide movements of both chest and arms in the first half of the record, followed by stillness in the second half. For each of the mentioned cases we present a

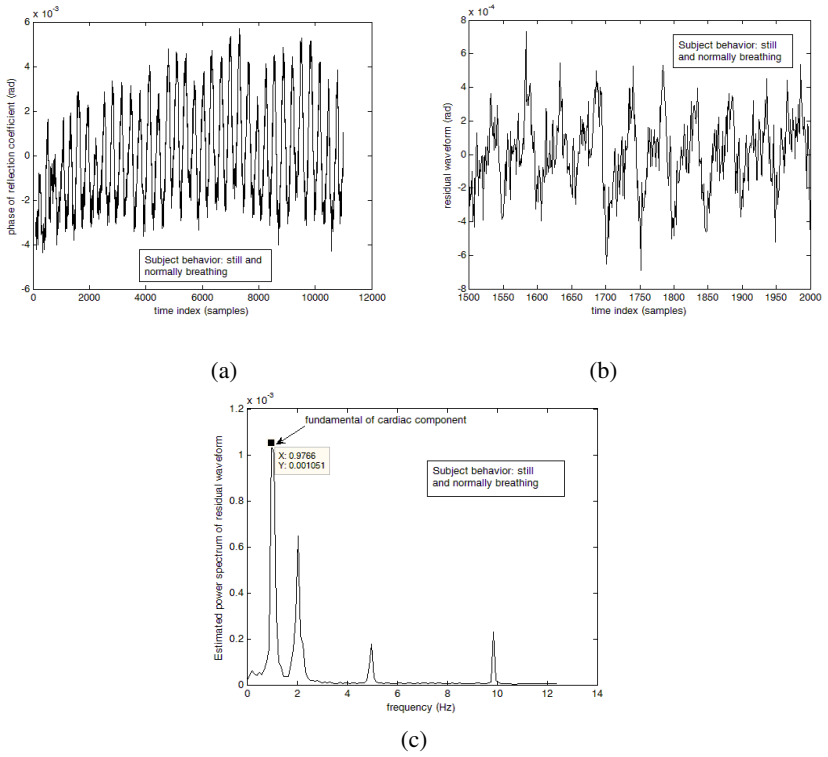

Fig. 3. Block #1: (a) diagram of the observed raw phase of the reflection coefficient; (b) diagram of the residual waveform (difference between the observed phase of the reflection coefficient and the output of the Kalman tracker); (c) Estimated power spectrum of residual waveform. $\sigma_p = 0.005$, $\sigma_n = 0.2$.

set of three figures: *a*) raw data vs. time for the whole block length, *b*) a fragment of the residual signal after cancellation of the slowly-varying component (i.e. the difference between the raw data and the Kalman filter output), *c*) finally, the averaged power spectrum estimate of the cited residual waveform. As for Block #2, a fourth figure is added (Fig. 4.d) showing the estimated spectrum of the residual signal in the second half of Block #2 where the subject is again still.

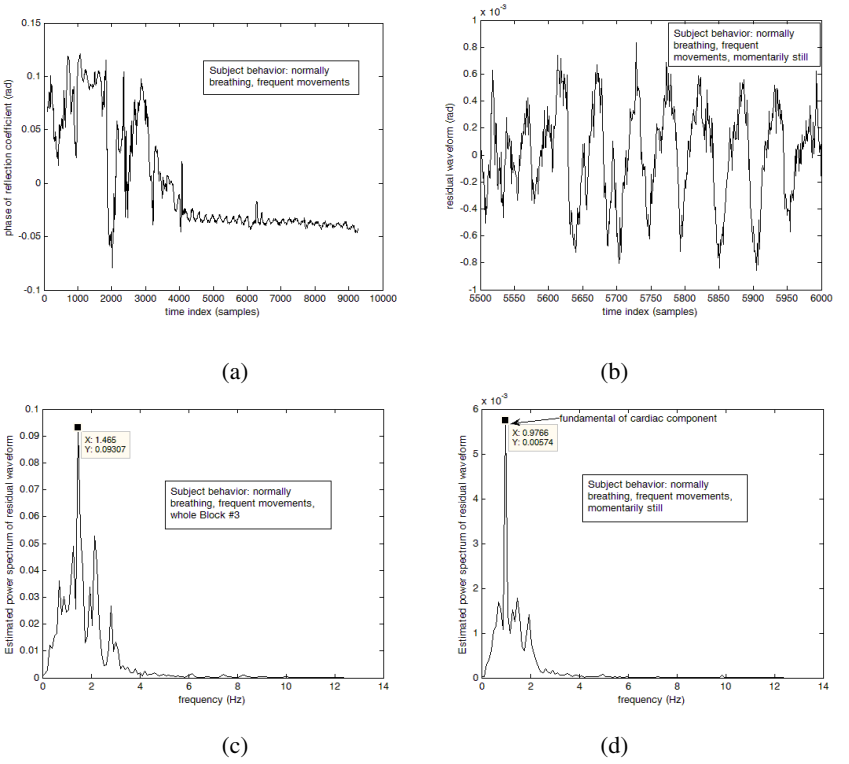

Fig. 4. Block #2: (a) diagram of the observed raw phase of the reflection coefficient (the impact of subject motion is visible in the first half of record); (b) diagram of the residual waveform in a segment where the subject is still; (c) estimated power spectrum of residual waveform (whole block); (d) estimated power spectrum of residual waveform starting from the sample with index 4300. $\sigma_p = 0.005$, $\sigma_n = 0.2$.

Inspection of the figures reveals that for Blocks #1 it is possible to neatly detect a narrowband spectral component centered on the cardiac rate, slightly less than 1 Hz (Figs. 3.c). Conversely, the same tone is not clearly visible in the spectrum obtained from the residual signal relative to the whole Block #2 (Fig. 4.c), while it pops up again if the elaboration is limited to the second part of the same record (Fig. 4.d). We also observe from Figs. 3.c and 4.d that the respiratory component is almost absent in the residual waveform, thus confirming the good accuracy in tracking and cancellation allowed by the Kalman filter. Other spectral components are visible in the

figures, notably the one falling in the vicinity of 2 Hz, most likely the first harmonic of the cardiac signal, whereas the peaks around 5 Hz and 10 Hz could not be unequivocally ascribed to a specific source. As for the curve in Fig. 4.c, produced from the entire Block #2, it is worth observing that it exhibits a main spectral peak around 1.5 Hz, that is not correlated to the cardiac component, its position on the frequency axis being too high. This peak is presumably to be ascribed to the random fluctuations of the residual waveform and also to the possible presence of other pseudo-periodic signal components in the first part of the record, affected by movements of the cooperating subject. A possible criterion to distinguish between a situation of this type with respect to the one in which the peak is actually produced by the cardiac activity could be based on the calculation of the mean squared value of the residual signal: this in fact appears to be far larger (around two orders of magnitude for the data processed in the examples, see Figs. 4.c-d) when the cooperating subject makes movements leading to large errors in the Kalman tracker. This seems one of the topics worth investigating further, in the search of safe criteria for automatic recognition of the signal segments where the above procedure is more likely to be successful.

4 Conclusions

Non-invasive sensing of cardiopulmonary activity is feasible by deploying an RF antenna close to the human thorax. Encouraging preliminary results have been obtained by applying Kalman filtering techniques to real data acquired through a low-cost RF device. Work is in progress to get a smaller device through integrated circuit technology, which can be integrated in a commercial communication device or a radio beacon, such as those carried on by rescue operators and miners [12].

References

1. Lin, J.C., Kiernicki, J., Kiernicki, M., Wollschlaeger, P.B.: Microwave apexcardiography. IEEE Trans. Microwaves Theory and Techniques 27, 618–620 (1979)
2. Lin, J.C.: Microwave sensing of physiological movement and volume change: a review. Bioelectromagnetics 13, 567–575 (1992)
3. Obeid, D., Sadek, S., Zaharia, G., El Zein, G.: Multitunable microwave system for touchless heartbeat detection and heart rate variability extraction. Microwave and Optical Technology Letters 52(1), 192–198 (2010)
4. Obeid, D., Sadek, S., Zaharia, G., El Zein, G.: Microwave doppler radar for heartbeat detec-tion vs electrocardiogram. Microwave and Optical Tech. Lett. 54(11), 2610–2617 (2012)
5. Serra, A.A., Nepa, P., Manara, G.: On-body antenna input-impedance phase-modulation induced by breathing and heart activity. In: URSI Intern. Symposium. IEEE Press (2008)
6. Serra, A.A., Nepa, P., Manara, G., Corsini, G., Volakis, J.L.: A single on-body antenna as a sensor for cardiopulmonary monitoring. IEEE Antenna and Wireless Propagation Letters 9, 930–933 (2010)

7. Fletcher, R.R., Kulkarni, S.: Clip-on Wireless Wearable Microwave Sensor for Ambulatory Cardiac Monitoring. In: 32nd International Conference of the IEEE EMBS, pp. 365–369 (2010)
8. Gagarin, R., Celik, N., Youn, H.S., Iskander, M.F.: Microwave Stethoscope: a new method for measuring human vital signs. In: IEEE International Symposium on Antennas and Propagation, pp. 404–407. IEEE Press (2011)
9. Celik, N., Gagarin, R., Youn, H.S., Iskander, M.F.: A Noninvasive Microwave Sensor and Signal Processing Technique for Continuous Monitoring of Vital Signs. IEEE Antenna and Wireless Propagation Letters 9, 930–933 (2011)
10. Tariq, A., Ghafouri-Shiraz, H.: On-body antenna for vital signs and hearth rate vari-ability monitoring. In: 2011 Loughborough Antenna & Propagation Conference, pp. 1–4 (2011)
11. Wikipedia, `http://en.wikipedia.org/wiki/Kalman_filter`
12. Dubrovka, R.F., Shirokov, I.B.: On-body antenna for the miners cardiac rhythm sensor. In: Antennas & Propagation Conference, Loughborough, pp. 581–584 (2009)